Available online at www.sciencedirect.com
SCIENCE DIRECT
Cement and Concrete Research 36 (2006) 740 – 748
Cement and Concrete Research

A new testing configuration for shrinkage cracking of shotcrete and fiber reinforced shotcrete

Christopher K.Y. Leung *, M. ASCE, Augustus Y.F. Lee, Raymond Lai

Department of Civil Engineering, Hong Kong University of Science and Technology, Clear Water Bay, Hong Kong

Received 5 October 2005; accepted 11 November 2005

Abstract

Shotcrete and fiber reinforced shotcrete are commonly employed to produce layers or linings with large surface area versus volume ratios. Restrained shrinkage cracking is hence an important concern. The common test set-up used for shrinkage cracking of concrete, with a ring specimen cast around a stiff steel form, is not applicable to shotcrete. A new testing configuration, consisting of a shotcrete specimen bonded to a steel I-section and angles, is therefore proposed. In this investigation, a finite element analysis was first performed to identify member sizes that provide a good compromise between the effectiveness of constraint and weight of steel members. Restrained shrinkage tests using this new configuration were performed for plain and fiber reinforced shotcrete. Despite the simplifying assumptions in the finite element analysis, the predicted degree of restraint is in reasonable agreement with test results. From the results, the proposed set-up is shown to be a practical and viable approach for investigating the shrinkage cracking behavior of shotcrete and fiber reinforced shotcrete.

Keywords: Shotcrete; Fiber reinforcement; Shrinkage; Finite element analysis

1. Introduction

The shotcreting process is commonly employed to produce cementitious layers and linings with large ratios of surface area to volume. When drying shrinkage is restrained by underlying material [1] or when differential shrinkage occurs within the shotcrete layer, cracking can occur. Shrinkage cracking can be controlled with the addition of fibers into the mix [2,3]. To facilitate the mix design of fiber reinforced shotcrete for practical applications, it is necessary to design a laboratory set-up that can assess the effectiveness of various mixes against shrinkage cracking. For concrete and fiber reinforced concrete, shrinkage cracking is often studied with the 'ring' test [4]. In this test, the concrete specimen is cast directly onto the inner steel ring. When shrinkage occurs, the restraint provided by the stiff steel ring will lead to the formation of radial cracks. This test configuration is found to be effective in inducing cracks and showing the difference among various compositions of FRC [5]. However, for shotcrete members, it is commonly accepted that material close to the sides of the formwork may not have the same compaction as materials farther away. If a ring specimen is prepared by shotcreting, cracking will occur in non-representative material right next to the form, and the result is difficult to interpret.

An alternative approach to perform the shrinkage test is as follows. A panel can first be prepared by shotcreting. Specimens are then cut at some distance from the sides, and bonded to an underlying substrate with sufficient stiffness. When shrinkage occurs, the restraint provided by the substrate will induce cracking in the specimens. The idea behind such an approach is certainly not new. To study the plastic shrinkage of concrete, Banthia et al. [6,7] employed steel reinforced high strength concrete plates to provide shrinkage restraint to young concrete specimens. For drying shrinkage, a test set-up for restraining plate specimens has been proposed by Pihlajavaara and Pihlman [8]. The challenge of such an approach lies in the selection of a proper member to provide the shrinkage restraint. If the underlying member is not stiff enough, cracking cannot be induced. On the other hand, if very large and heavy members are employed to restrain the shrinkage, it becomes highly uneconomical and inconvenient when a large number of tests need to be performed.

* Corresponding author.
E-mail address: ckleung@ust.hk (C.K.Y. Leung).

0008-8846/$ - see front matter © 2005 Elsevier Ltd. All rights reserved.
doi:10.1016/j.cemconres.2005.11.018

In the present investigation, steel I-beam is employed as the restraining substrate. Based on the results from finite element analysis, the size of the I-beam and the shotcrete specimen are chosen to ensure that (i) there is sufficient restraint to induce cracking, and (ii) the I-beam is small and light enough to enable the convenient performance of a large number of tests. To demonstrate the applicability of the proposed set-up, shrinkage cracking experiments are performed with plain shotcrete and three different compositions of fiber reinforced shotcrete. By comparing the shrinkage of restraint specimens to that of free specimens, the degree of restraint is also calculated to verify the finite element results.

2. Design of the novel testing configuration

To come up with the appropriate testing set-up, engineering judgment is complemented with numerical analysis. As will be elaborated below, the numerical analysis is approximate in nature, as the main purpose is to come up with reasonable dimensions for the set-up, rather than to obtain the exact stress distribution during the test. The proposed testing configuration is illustrated in Fig. 1. The lower surface of a shotcrete specimen is epoxy bonded to a steel I-section, and its ends are bonded to steel angles that are welded to the I-section. Along the bottom of the specimen, an air gap (with no epoxy) is left for the following reason. For a specimen constraint in the manner shown by Fig. 1, when uniform shrinkage occurs, the tensile stress is maximum at the bottom of the specimen and decreases towards the upper surface. If the lower surface is completely bonded to the I-section, when a crack forms at the bottom of the specimen, the glue may prevent it from opening and propagating. As a result, the observation of cracking may be delayed. With an air gap left in the middle, the uniformity of the stress distribution is significantly improved (although the stress may still be slightly higher at the bottom). With a more uniform stress distribution, and without the epoxy glue at the bottom, cracks can propagate and open easily, and are hence more readily observable. It should be noted that restrained shrinkage specimens with part of the member 'free' or unbonded have been previously employed by Pihlajavaara and Pihlman [8] and Paillere et al. [9].

3. Finite element modeling

The model for the testing set-up, together with its boundary conditions, is illustrated in Fig. 2. Due to symmetry, only half of the set-up is modeled. The appropriate boundary condition at the plane of symmetry is introduced with one hinge and a number of rollers that only allow displacement in the vertical direction. For shrinkage testing to be conveniently performed, we assume that the set-up can be placed directly on the floor or on shelves inside a room with controlled temperature and humidity. Under such a condition, the actual boundary condition along its bottom surface is not very well defined. For the purpose of choosing the dimensions for the set-up, two limiting cases were considered to obtain upper and lower bound estimates of the restraint. In Fig. 2, a case with a roller at the edge of the I-section steel base is shown. The purpose of the roller is to prevent any 'uplifting' at the end of the steel base. Its incorporation stiffens up the base, and therefore provides an upper bound estimate of the restraint on the specimen. To give a lower bound value, the roller is removed. Because the dead weight of the steel member is not considered in the numerical analysis, the steel base is free to deform upwards as the specimen shrinks. By neglecting the downward bending effect from the dead weight, the effectiveness of restraint is underestimated. As will be shown, these two bounds are not very far apart from one another, and can hence provide useful guidelines for designing the set-up.

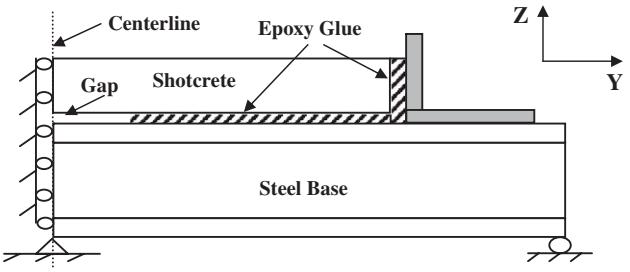

Fig. 2. Model with hinge support for the calculation of upper bound values of restraint.

To perform a finite element analysis, the three dimensional system was first converted into an equivalent 2-D model (as in Fig. 2). This is acceptable as we are mainly interested in the variation of stresses along the length of the specimen. To start off the analysis, initial dimensions have to be assumed. The size of the shotcrete specimen is taken to be $500 \times 100 \times 100$ mm. The steel angle is taken to be of the same width ($W = 100$ mm). For the steel base, the sizes of commonly available I-sections are employed. Since the I-section has variable width along its depth, effective values have to be obtained for input into the two-dimensional model. Specifically, the section is divided into

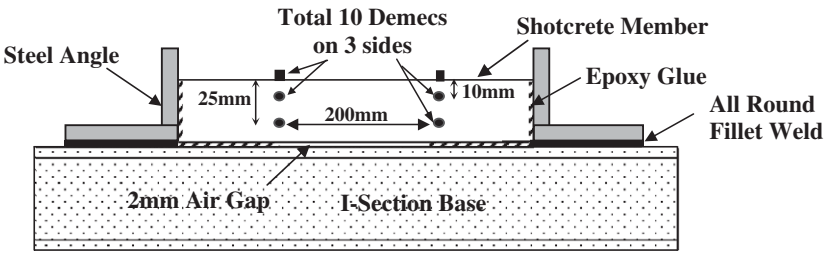

Fig. 1. The proposed testing configuration.

three parts, the top flange, the web and the bottom flange. To convert the I-section into an equivalent section of uniform width (W) that is consistent with the shotcrete specimen, the Young's Modulus for the flange (E_{flange}) and web (E_{web}) are modified as:

$$E_{\text{flange}} = \frac{B}{W} E_{\text{steel}} \tag{1}$$

$$E_{\text{web}} = \frac{t}{W} E_{\text{steel}} \tag{2}$$

where B is the width of the flange and t is the thickness of the web. The E values of steel and concrete are taken as 200 and 30 GPa, respectively. In the model, the epoxy layer is assumed to be 2 mm in thickness and its E value is taken to be 7.5 GPa. These values are typical for the filled epoxy employed in our laboratory.

In the finite element analysis, eight-node elements were used throughout. A typical mesh is illustrated in Fig. 3. The length to width (l/w) ratio of each element is practically limited to five. If the l/w ratio is too large, the element may be heavily distorted to cause large errors in the analysis [10]. All the materials are assumed to be homogeneous and isotropic, with Poisson's ratios equal to 0.2. Because the width of the set-up is small, the 2-D analysis is performed under plane stress conditions.

To simulate drying shrinkage in the model, the shotcrete specimen is modelled as a thermal type material whereas the other materials are considered elastic (see Table 1). The shrinkage strain can hence be represented by an equivalent thermal contraction of $\alpha\Delta T$, with α being the assumed thermal expansion coefficient and ΔT the change in temperature. In reality, the shrinkage strain may vary over the depth of the specimen, so a varying ΔT is required. Moreover, creep will reduce the stress induced by restrained shrinkage, and this effect cannot be captured in an elastic analysis. However, since the purpose of the analysis is to select the appropriate sizes of shotcrete specimen and steel members, rather than obtaining accurate stress distributions in the specimen when shrinkage occurs, it suffices to assume uniform shrinkage (represented by uniform ΔT) and elastic properties in the model.

If the specimen is fully constrained, the induced tensile strain is given by

$$\varepsilon_{\text{FR}} = \alpha \Delta T. \tag{3}$$

In the present testing configuration, since stresses along the vertical direction of the specimen are very small, the maximum possible induced longitudinal stress can be taken as the product of ε_{FR} and the material's Young's modulus.

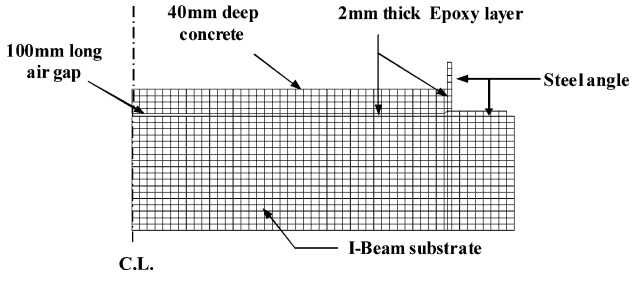

Fig. 3. A typical finite element mesh for the analysis.

Table 1
Material properties input for the finite element model

Material	Type	E (GPa)
Flange	Elastic	E_{flange}
Web	Elastic	E_{web}
Epoxy glue	Elastic	7.5
Steel angle	Elastic	200
Concrete	Thermal	30

In the analysis, α and ΔT are taken to be 1×10^{-6}/°C and -100 °C. Under perfect restraint (i.e., 100% of the shrinkage is restrained), the induced tensile strain ε_{FR} is 1×10^{-4}. In the actual situation, the restraint may not be perfect so the induced strain is below this maximum value. Also, along the length and depth of the specimen, the induced strain is not uniform. In the simulation results shown in the following sub-sections, all the strain values are normalized by ε_{FR} to obtain the percentage of maximum restraint (or restrained percentage). The effectiveness of restraint for various cases is then compared.

3.1. Determination of steel base size

The first set of simulation aims at determining the size of the steel base. To start the analysis, the $500\times100\times100$ mm shotcrete specimen is bonded to a 800 mm long steel base, with steel angles $100\times100\times15$ mm fixed at its two ends. In the selection of steel member size, as well as the determination of specimen size in the next sub-section, we assume that there is no air gap along the bottom of the specimen. The air gap will be introduced at the last stage and its size is determined from an additional set of simulations.

In the analysis the restraint provided by various types of steel section are compared. Fig. 4 shows the results for the upper bound case (with a roller at the edge of the I-section). For four common types of standard I-section, Fig. 4(a) shows the variation of restraint percentage over the depth at the mid-section of the shotcrete member, while Fig. 4(b) shows the variation on the upper surface along the specimen length. The corresponding lower bound results are shown in Fig. 5(a) and (b). As shown in the figures, the percentage of restraint decreases from the bottom to the top of the specimen. To come up with appropriate dimensions for the experimental set-up, we will focus on the value of restrained percentage along the upper surface of the specimen, which is usually the smallest over the section. If even this smallest value is sufficiently high, we know that the specimen is effectively restrained by the steel member.

As expected, for the larger I-sections that are stiffer, the difference between upper and lower bound results is smaller. From the figures, even the largest member, weighing 388 kg/m, can only provide 60% of the maximum possible restraint. This result implies that the depth of the concrete specimen should be reduced. However, based on Figs. 4 and 5, one can determine an appropriate type of steel section before proceeding to look at other parameters.

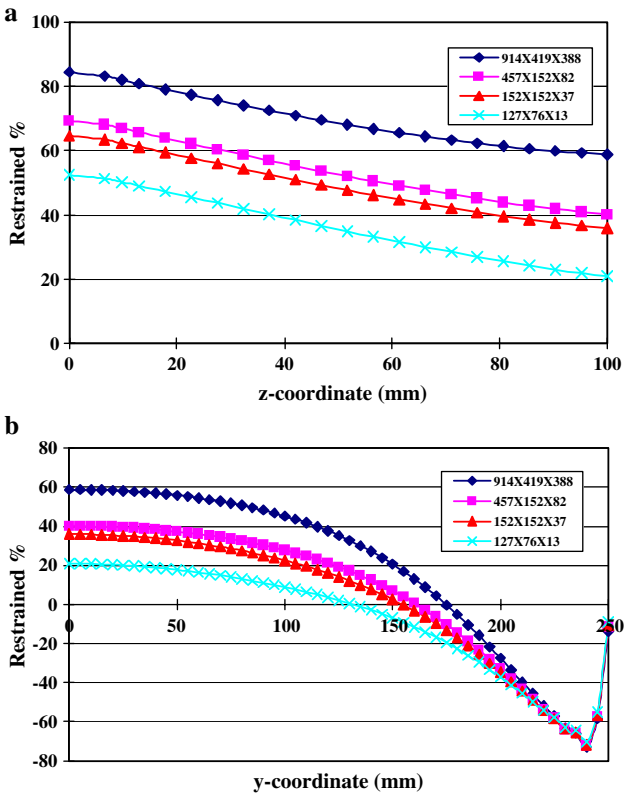

Fig. 4. (a) Variation of restraint over the specimen depth at the mid-section (upper bound case). (b) Variation of restraint along upper surface of specimen (upper bound case).

From Fig. 4(a) and (b), which show the upper bound values, the $457 \times 152 \times 82$ kg/m section is found to induce only slightly higher tensile stress than the $152 \times 152 \times 37$ kg/m section although the former is much deeper than the latter. In this case, since bending of the I-section is resisted by rollers at the bottom corners (see Fig. 2), the shrinkage-induced stress in the steel member is mainly compressive. Compressive stress is transmitted directly to the upper flange and then from the web to the lower flange. For a deep (but slender) web, the stress cannot be effectively transferred to the lower flange. As a result, similar values of restrained percentage are obtained for the $457 \times 152 \times 82$ kg/m and $152 \times 152 \times 37$ kg/m sections. For the lower bound values shown in Fig. 5(a) and (b), the $457 \times 152 \times 82$ kg/m section performs much better than the $152 \times 152 \times 37$ kg/m section. This is because the I-section is free to bend in this case. The deeper section with a much higher bending stiffness will then provide a significantly better restraint. The upper and lower bound results suggest the selection of different steel section types. However, in view of the fact that the $152 \times 152 \times 37$ kg/m section is lighter in weight and more convenient to handle, we decide to use this section for further analysis.

Theoretically speaking, the length of steel section beyond the specimen (which is $0.5*(800-500)$ or 150 mm in the present case) is another parameter that can be varied. However, the percentage restraint is expected to be insensitive to this parameter, because the part of steel section outside the specimen should not have a large effect on the restraint. This argument has been confirmed by numerical simulations. The results are not shown in this paper but can be found in Lai [11].

3.2. Determination of shotcrete specimen size

According to the results given in Figs. 4(b) and 5(b), the maximum restraint occurs at the mid-section along the length. To study the effect of specimen thickness on the restrained percentage, we will focus on values along the mid-section. In Table 2, for both the upper and lower bound cases, the values of restrained percentage at the top and bottom surfaces of the specimen as well as the average restrained percentage (calculated as the mean value over the whole section) are shown. As expected, the percentage of restraint is higher for smaller specimen depth and reaches a mean value of 70% to 82% (lower and upper bounds) for a depth of 40 mm. Practically, it is not easy to prepare specimens thinner than 40 mm as the shotcrete panel becomes vulnerable to damage during handling, and the error in thickness will be relatively large. Therefore, the 40 mm depth shotcrete specimen is considered appropriate.

Simulations have also been performed to see how the length of the shotcrete specimen may affect the restraint. Representative results, obtained for 500 and 800 mm specimens are compared in Fig. 6. The lengths of steel base for the

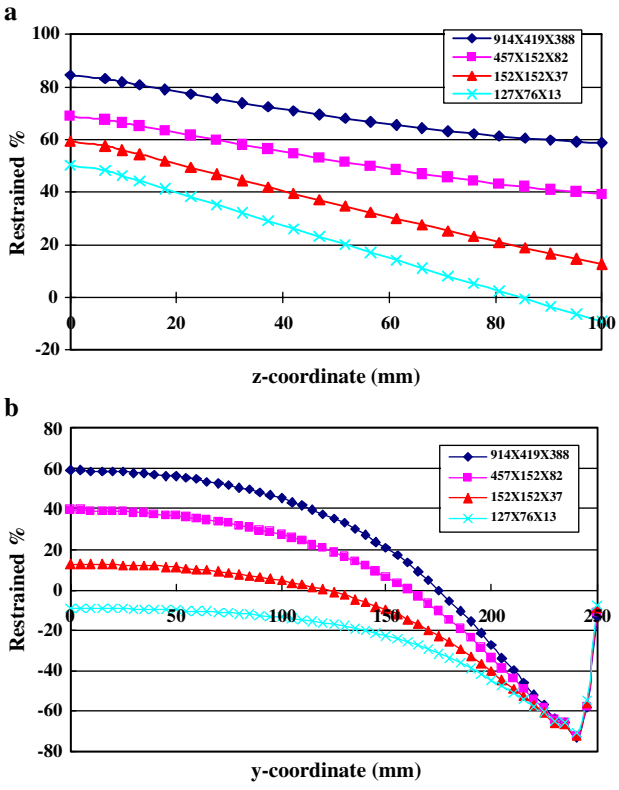

Fig. 5. (a) Variation of restraint over the specimen depth at the mid-section (lower bound case). (b) Variation of restraint along upper surface of specimen (lower bound case).

Table 2
Effect of specimen thickness on upper and lower bound values of restraint at the mid-section (shotcrete specimen length = 500 mm)

Thickness (mm)	Upper surface restrained percentage (upper bound)	Upper surface restrained percentage (lower bound)	Bottom surface restrained percentage (upper bound)	Bottom surface restrained percentage (lower bound)	Mean upper bound restraint percentage	Mean lower bound restraint percentage
100	35.9	12.8	64.5	59.4	50.1	36.2
80	52.7	29.1	67.7	61.0	60.2	44.9
60	69.1	47.8	73.5	65.5	70.8	57.1
40	82.5	66.7	81.8	73.9	82.1	70.2

two specimens are respectively 800 mm and 1 m. Comparing with the 500 mm specimen, the 800 mm specimen has a longer length of contact area for stress transfer, and thus exhibits a higher restrained percentage. More importantly, for the 500 mm case, the restrained percentage stays at a high value (close to the maximum) only over a relative small region around 70 to 100 mm from each side of the mid-section. For the 800 mm, the percentage of restraint decreases slowly over a much larger region (up to 200 mm from each side). Since shotcrete is not homogeneous, the existence of high strain over a larger region will increase the chance for crack formation. A $800 \times 100 \times 40$ shotcrete specimen is hence used for further study.

3.3. Determination of steel angle size

As shown in Fig. 2, steel angles are welded on the top flange of steel I-section to provided restraints to the shotcrete specimen at its ends. Two sizes of steel angle, $75 \times 75 \times 6$ kg/m and $100 \times 100 \times 15$ kg/m have been compared in the finite elements analysis. The results [11] show that they produce almost identical values of restrained percentage at the mid-section of the shotcrete specimen. The implication is that either of these angles is stiff enough so the smaller one is chosen.

3.4. Size of gap between specimen and steel base

With the specimen and steel member dimensions determined above, different gap lengths (0, 200, 400 and 600 mm) are introduced in the analysis. The variation of restrained percentage along the upper surface is shown in Fig. 7. Both upper and lower bound results are shown. Table 3 shows the effect of gap length on the restrained percentage along the mid-section. With the increase in size of the air gap, the maximum induced tensile stress is decreased and so is the restrained percentage. It is because the contact area between the concrete specimen and the steel I-section is reduced. With a shorter length for stress transfer, the restraint condition becomes less effective.

From Fig. 7, one can observe that the restrained percentages are essentially uniform within the gap region. As discussed above, this is desirable as cracks may form anywhere in the region. Near the junction between the bonded and unbonded parts of the specimen, a high tensile stress exists and the value may be higher than that within the gap region. However, as long as this value is not too much higher than the stress in the gap region, it is unlikely for the specimen to exhibit a weak point in the small region over which this higher stress exists. Actual cracking will then not be associated with this stress. From the numerical results, we can see that the restrained percentage for no gap and 200 mm gap are very close to each other, while higher gap lengths result in more significant decrease in the percentage of restraint. Also, the 200 mm gap case does not show a particularly high stress outside the region of the gap. Based on the analysis, a gap length of 200 mm is chosen for experimental work. According to the results, the mean

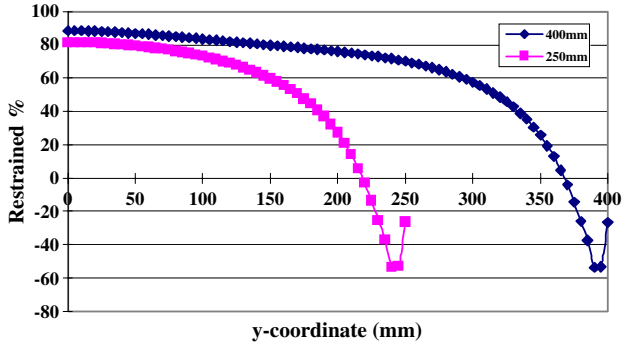

Fig. 6. Effect of shotcrete specimen length on variation of restraint along surface of specimen (upper bound values).

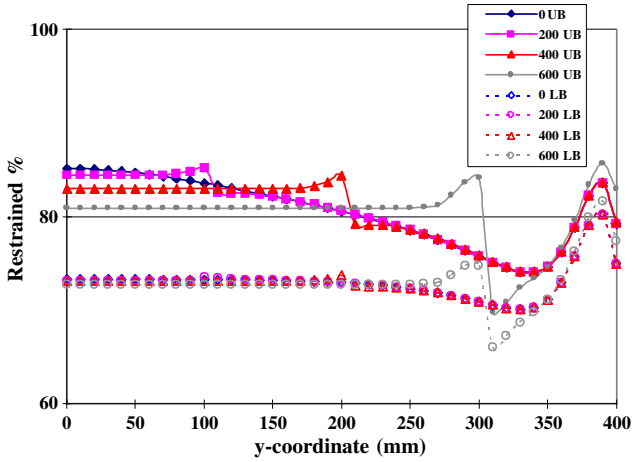

Fig. 7. Effect of air gap length on variation of restraint along upper surface of specimen (UB: upper bound, LB: lower bound).

Table 3
Effect of gap length on upper and lower bound values of restraint at mid-section (shotcrete specimen length=800 mm, depth=40 mm)

Gap length (mm)	Upper surface restrained percentage (upper bound)	Upper surface restrained percentage (lower bound)	Bottom surface restrained percentage (upper bound)	Bottom surface restrained percentage (lower bound)	Mean upper bound percentage of restrain	Mean upper bound restraint percentage
0	88.5	65.0	85.1	73.3	86.8	69.2
200	84.6	65.0	84.4	73.1	84.5	69.1
400	80.5	64.3	83.0	73.1	81.7	68.7
600	72.2	59.4	81.0	72.7	76.6	66.1

restrained percentage in the central portion would lie within the range of 69.1% and 84.5%.

4. Final configuration

According to the above step-by-step numerical analyses, a final configuration of the test set-up is developed. A 1000 mm long $152 \times 152 \times 37$ kg/m steel I-section is used as the steel base. The steel angle size is $75 \times 75 \times 6$ kg/m. The shotcrete specimen is chosen to be $800 \times 100 \times 40$ mm. A gap of length 200 mm at the mid-span is left between the concrete specimen and the steel I-section. The total weight of the steel fixture and shotcrete specimen is below 50 kg, which is not difficult to handle by two persons in the laboratory.

5. Experimental program for verification of the set-up

In the above, a testing configuration for shrinkage cracking was designed with the help of finite element analysis. To assess the applicability of this set-up in practice, restrained shrinkage test was performed on shotcrete specimens of various compositions. Four different sets of specimens were prepared with the wet-shotcreting process. The mix proportion of cementitious matrix was similar in all cases (Table 4). One set of specimens contained no fiber. The other three sets were prepared respectively with 0.5% polypropylene (PP), 0.5% polyvinyl alcohol (PVA) and 0.5% steel (ST) fibers. All the constituents were first mixed in large portal mixers before pumping into a pipeline, and sprayed through a nozzle to form panels $1200 \times 1200 \times 40$ mm in size. The shotcreted panels were kept wet by curing agent and covered with plastic sheets for one day. Then, specimens with size of $800 \times 100 \times 40$ mm were sawn cut from these panels. For each mix, six specimens were obtained—three for restrained shrinkage test while the other three were left to shrink freely in the environmental room. Based on the difference in shrinkage strain measured on the restrained and free specimens, the experimental restrained percentage can be deduced.

To provide shrinkage restraint, each shotcrete specimen was bonded with epoxy adhesive to the proposed steel setup (Fig. 1). To encourage cracking on the upper surface, which is easier to observe, the sides of the specimen were coated with vacuum grease to prevent water loss. The air gap at the bottom was also sealed with rubber sealant. For direct comparison, the sides and bottom surface of the free specimens were also sealed in a similar manner.

To monitor shrinkage strain on the specimen, Demac gauge targets (or simply called Demacs) were placed on the upper surface, as well as on the sides, at distances 10 and 25 mm from the top (Fig. 1). Caution should be paid not to fix Demacs too close to the upper flange of the steel beam. Otherwise, there will be insufficient space for readings to be taken. On the unrestrained specimens, Demacs were also attached at exactly the same locations to monitor the free shrinkage behaviour.

Table 4
Composition of cementitious matrix for all shotcrete specimens

Cement	Stone fine	River sand	Water	Micro silica
430 kg	1097 kg	365 kg	275 kg	35 kg

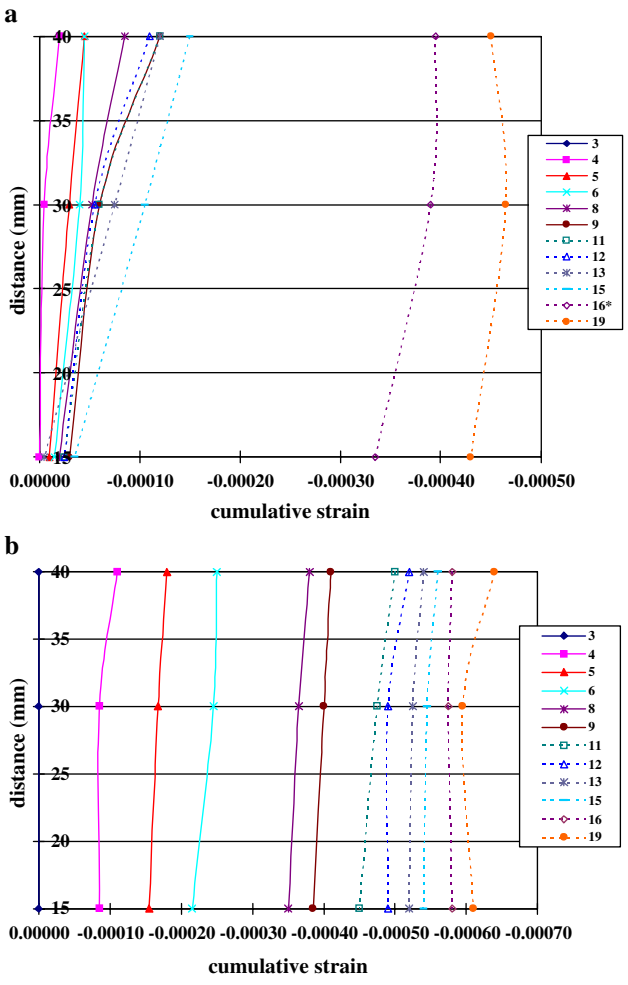

Fig. 8. (a) Typical variation of strain with time for a restrained specimen (0.5% PP fiber). (b) Typical variation of strain with time for a free specimen (0.5% PP fiber).

To induce drying shrinkage, the restrained and unrestrained specimens were placed in an environmental room at 50% relative humidity and 28 °C to accelerate the shrinkage effect. In the room, the temperature variation was within +1 °C, while the relative humidity was maintained within ±5%. After the specimens were bonded to the steel fixture, we allow one day for the epoxy to harden before the specimens were placed in the environmental room. The first Demac reading was hence taken at Day 3, which was two days after shotcreting. On every subsequent working day, the strain values across the depth of the specimen (at the levels of the Demacs) were measured and visual inspection for cracks were also carried out.

6. Test results

The first objective of the work is to see if the steel members are indeed stiff enough to induce shrinkage cracks. For the 12 specimens (4 compositions × 3 specimens each) under restrained shrinkage, cracks could be visually observed on 11 of them. For the uncracked member (which is reinforced with PVA), the Demac readings indicated that it only shrunk a little bit less than corresponding free specimens. This is probably due to poor workmanship that resulted in poor bonding between the shotcrete specimen and the steel member. While visual inspection could clearly reveal the occurrence of cracking, to find the time when cracking initiated, a more objective method was employed. On each working day, the strain values on both restrained and free members were measured with the Demac gauge. Typical variations of strain versus time for restrained specimens are shown in Figs. 8(a) and 9(a). The x-axis indicates the strain value (−ve for shrinkage) and the y-axis denotes the distance from the bottom of the specimen. The figure therefore shows the variation of strain with time over the upper part of the specimen (15 to 40 mm from the bottom). Note that the point at 15 mm (or 25 mm) from the bottom represents the average of two readings taken from both sides of the specimen. From Fig. 8(a), the magnitude of strain increases slowly up to the 15th day, and then jumps to a much higher value on the 16th day. Such a 'jump' can also be observed in Fig. 9(a), but in an opposite direction, with the strain value going from positive to negative between the 13th and the 16th day. The occurrence of the 'jump' can be explained by the formation of a crack in the specimen, causing a sudden change in strain. The direction of the change (positive or negative) depends on whether the crack is formed within or outside the Demac gauge targets. From our test results, the 'jump' in strain was observable in every one of the restrained specimens, and always occurred before the crack could be observed by eye. On the other hand, for the free specimens, with typical shrinkage behavior shown in Figs. 8(b) and 9(b), cracking did not occur and the 'jump' in strain was never observed.

Another objective of the work is to see if the degree of restraint (or restrained percentage) determined from the tests is similar to predicted values from the finite element analysis. Since we are interested in the restraint imposed on the specimen when cracking is about to occur, the strain values

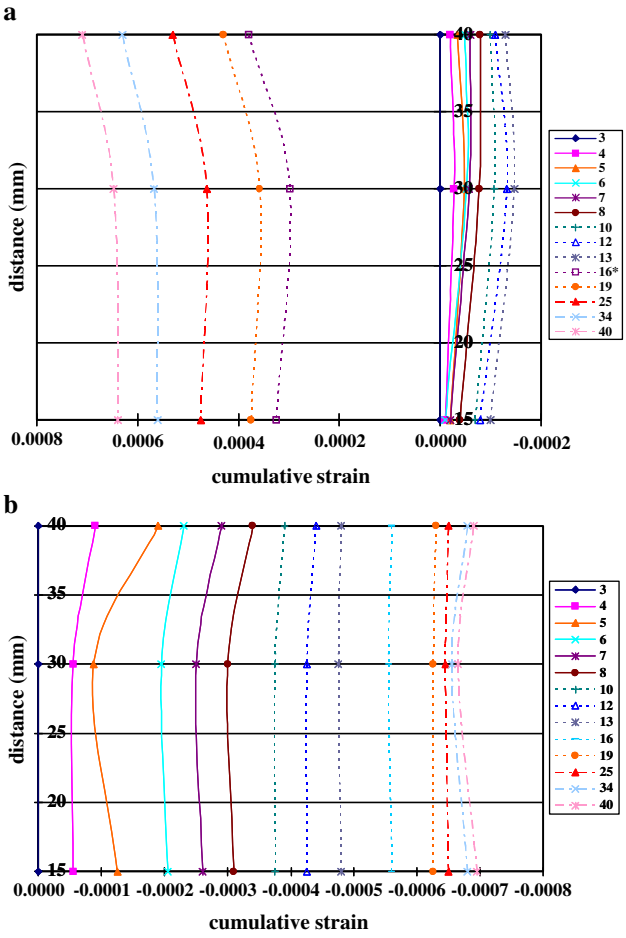

Fig. 9. (a) Typical variation of strain with time for a restrained specimen (0.5% PVA fiber). (b) Typical variation of strain with time for a free specimen (0.5% PVA fiber).

for the restrained and free specimens ($\varepsilon_{restrain}$ and ε_{free}) are taken as the cumulative strain up to the last day before cracking with available results. For example, from Figs. 8(a) and 9(a), cracking was found to occur at the 16th day for both cases. The last days with available data were the 15th and 13th day, respectively. To find the restrained percentage, the strain values measured at 15, 25 and 40 mm from the bottom are averaged in the following manner. Taking the distance from the bottom to be the x-coordinate, and the strain values to be the y-coordinate, a quadratic equation is fitted through the three points where strain is measured. Based on the equation, the average value over the top 25 mm of the specimen can be calculated. This 'averaging' is performed for both restrained and free specimens, and the results for all the specimens are given in Table 5. It should be noted that the three restrained specimens with the same composition do not necessarily crack at the same time. To calculate the percentage of restraint for each specimen, the free shrinkage strain (ε_{free}) was taken to be the mean value (for three free specimens) at the corresponding time when $\varepsilon_{restrain}$ was obtained.

To compare numerical and experimental results on the restrained percentage, the average restrained percentage in the upper part of the specimen (15 to 40 mm from the bottom) is

Table 5
Restrained percentage for the various specimens

Shotcrete mix	Last day before cracking	Shrinkage of restrained specimen $\varepsilon_{restrain}$ (10^{-6})	Shrinkage of free specimen ε_{free} (10^{-6})	Shrinkage difference $\Delta\varepsilon=\varepsilon_{free}-\varepsilon_{restrain}$ (10^{-6})	Restrained percentage $\Delta\varepsilon/\varepsilon_{free}$ (%)
Concrete	5	−17	−103	−86	84
	5	−11	−103	−92	89
	11	−26	−395	−369	93
				Mean: −182	Mean: 89
	8	−65	−204	−139	68
0.5% PVA	13	−136	−477	−341	72
				Mean: −240	Mean: 70
	8	−97	−442	−345	78
0.5% ST	8	−154	−442	−288	65
	8	−70	−442	−372	84
				Mean: −335	Mean: 76
0.5% PP	6	−23	−214	−191	89
	12	−83	−455	−372	82
	15	−93	−545	−452	83
				Mean: −338	Mean: 85

obtained from the finite element results. The upper and lower bound values are respectively 67.8% and 84.5%. Note that these values are not necessarily the same as those given in Table 3, which are obtained by averaging over the full depth. From the results in the last column of Table 5, the mean restrained percentage for all the fiber reinforced specimens lies within the upper and lower bounds. The plain shotcrete specimens are found to have a higher percentage of restraint than the upper bound. This can be explained by the fact that shrinkage is non-uniform over the specimen. As the part with less shrinkage (which is the lower part) tends to restrain the part that shrinks more (which is the upper part), shrinkage restraint is not just provided by the steel member, but also by the specimen itself. A higher restrained percentage than the numerical results is hence possible. Considering all the experimental results together, the mean restrained percentage ranges from 70% to 89%, which is in reasonable agreement with the numerical bounds of 67.8% and 84.5%. Based on the comparison, the following statement can be made. Despite all the simplifying assumptions in the elastic finite element analysis, it can provide a reasonable prediction of the restraint effectiveness, and is hence useful in the design of testing set-up for restrained shrinkage cracking.

Before closing, a comment should be made on the much higher free shrinkage of the steel fiber reinforced shotcrete specimens in comparison to the others. As a quality control measure, concrete cylinders have been prepared with each of the mixes (before they were pumped and shot). The 28-day compressive strength of the steel fiber reinforced shotcrete reached 58 MPa, while the value for the other mixes ranged from 36.8 to 44.5 MPa. Since the compressive strength is insensitive to the incorporation of a small volume fraction of fibers, the test results reflect plausible variations in the matrix composition. Thus, we believe that there were some inconsistencies in the batching process, giving rise to a higher cement content but lower aggregate content in the mix with steel fibers. With a lower water/cement ratio, the compressive strength is increased. However, since shrinkage is more sensitive to the aggregate content than the w/c ratio [12], a reduced aggregate content would lead to a significant increase in shrinkage.

7. Conclusions

In this paper, a new testing configuration to investigate the drying shrinkage of FRS is proposed. With the help of a finite element analysis, the dimensions of the set-up and the shotcrete specimen are determined to satisfy the dual requirements of effective restraint to shrinkage and low weight to make testing convenient. Experiments performed on plain shotcrete and three different kinds of fiber reinforced shotcrete indicate that the proposed testing configuration is effective in inducing shrinkage cracking. Also, the degree of restraint, obtained from the difference in strain measured on restrained and free specimens under the same environment, is found to be in reasonable agreement with finite element predictions. From the present investigation, two major conclusions can be drawn. Firstly, the elastic finite element analysis, while being simple, can provide reasonable estimates of strain in restraint concrete member. It is hence a useful tool for the design of testing set-up. Secondly, the new testing configuration developed in this work is practical and viable for investigating the shrinkage behavior of shotcrete and fiber reinforced shotcrete.

Acknowledgements

Financial support of the work by the Hong Kong Research Grant Council, under CERG UST6225/00E, as well as the assistance of Gammon Skanska in preparing the shotcrete specimens, are gratefully acknowledged.

References

[1] M. Asad, M.H. Baluch, A.H. Al-Gadhib, Drying shrinkage stresses in concrete patch repair system, Magazine of Concrete Research 49 (181) (1997) 283–293.
[2] P.N. Balaguru, S.P. Shah, Fiber Reinforced Cement Composites, McGraw Hill, New York, 1992.

[3] R.N. Swamy, H. Stravrides, Influence of fiber Reinforcement on restrained shrinkage and cracking, ACI Materials Journal 76 (3) (1979) 443–460.
[4] P.A. Dahl, Plastic Shrinkage and Cracking Tendency of Mortar and Concrete Containing Fiber Mesh, Report No. STF65A85039, SINTEF Div. FCB, Trondheim, Norway, 1985.
[5] M. Grzybowski, S.P. Shah, Shrinkage cracking of fiber reinforced concrete, ACI Materials Journal 87 (2) (1990) 138–148.
[6] N. Banthia, C. Yan, S. Mindess, Restrained shrinkage cracking in fiber reinforced concrete: a novel test technique, Cement and Concrete Research 26 (1) (1996) 9–14.
[7] N. Banthia, C. Yan, Shrinkage cracking in polyolefin fiber-reinforced concrete, ACI Materials Journal 94 (1997) 492–499.
[8] S.E. Pihlajavaara, E. Pihlman, Results of Long-Term Deformation Tests of Glass Fiber Reinforced Concrete, NORDFORSK-FRC Project 1974-76, Delrapport, Technical Report Center of Finland, Otaniemi, 1978.
[9] A.M. Paillere, M. Buil, J.J. Serrano, Effect of fiber addition on the autogeneous shrinkage of silica fume concrete, ACI Materials Journal 86 (2) (1989) 139–144.
[10] K.J. Bathe, Finite Element Procedures, Prentice Hall, New York, 1996.
[11] T.K. Lai, Effects of Fiber Addition on Various Properties of Shotcrete and Concrete, M.Phil Thesis, Hong Kong University of Science and Technology, 2002.
[12] A.M. Neville, Properties of Concrete, 4th Edition, Longman, 1995.